ELSEVIER

Physica D 105 (1997) 226–252

PHYSICA D

Chaotic principle: An experimental test

F. Bonetto [a], G. Gallavotti [b,*], P.L. Garrido [c]

[a] *Matematica, I[a] Università di Roma, P.le Moro 2, 00185 Roma, Italy*

[b] *Fisica, I[a] Università di Roma, P.le Moro 2, 00185 Roma, Italy*

[c] *Instituto Carlos I de Fìsica Teórica y Computacional, Universidad de Granada, E-18071 Granada, Spain*

Received 20 May 1996; accepted 5 December 1996

Communicated by H. Müller-Krumbhaar

Abstract

The chaotic hypothesis discussed in Gallavotti and Cohen (1995) is tested experimentally in a simple conduction model. Besides a confirmation of the hypothesis predictions the results suggest the validity of the hypothesis in the much wider context in which, as the forcing strength grows, the attractor ceases to be an Anosov system and becomes an Axiom A attractor. A first text of the new predictions is also attempted.

Keywords: Chaotic hypothesis; Reversibility; Entropy; Dynamical systems

1. Introduction

A principle holding when motions have an empirically chaotic nature was introduced in [1]:

Chaotic hypothesis: A many-particle system in a stationary state can be regarded as a smooth dynamical system with a transitive [1] Axiom A global attractor for the purpose of computing macroscopic properties. In the reversible case it can be regarded, for the same purpose, as a smooth transitive Anosov system.

For an informal discussion of the properties of Anosov systems relevant for this work, in particular for the "Boltzmanian representation" of the SRB distribution possible for them, see [1,2]. See [3,4] for a general discussion on the basic geometrical ideas and [5–8] for the original and complete descriptions of the mathematical notion and properties of Anosov and Axiom A systems.

The results of this work mainly concern the reversible Anosov case: in the concluding remarks we discuss various questions related to reversibility and to the Axiom A cases. Therefore the part of the hypothesis that refers

* Corresponding author.

[1] The notion of transitivity used in [1], and in the related ones, is that the stable and unstable manifolds of each point of the attractor are dense on the attractor.

PII S0167-2789(97)00007-9

to reversible systems is essential for our applications. It can be rephrased in various ways and, by doing so, one gains some insights into its meaning: see Section 6.

This implies that macroscopic time averages are described by a probability distribution μ on the "phase space" $\mathcal{C}$ of *observed events*, also called *timing events* (which could be, for instance, the occurrence of a microscopic binary "collision"). The time evolution, or the *dynamics*, is a map S of $\mathcal{C}$ into itself. The map S is derived from the flow Q_t that solves the differential equations of motion of the system: the timing events $\mathcal{C}$ have to be thought as a surface transversal to the flow and if $t(x)$ is the time between the timing event x and the successive one Sx it is $Q_{t(x)}x = Sx$. Note that the points $Q_t x$ *are not* timing events (i.e. they are not in $\mathcal{C}$) for the intermediate times $0 < t < t(x)$.[2] We call Q_t the *continuous time evolution* and S the *discrete* time evolution.

Existence of the distribution μ is assumed, in general, as stated by the following (extension) of the zeroth law [9] giving a global property of motions generated by initial data chosen randomly with distribution μ_0 *proportional to the volume* measure on $\mathcal{C}$.

Extended zeroth law: A dynamical system $(\mathcal{C}, S)$ modeling a many-particle system (or a continuum such as a fluid) describes motions that admit a statistics μ in the sense that, given any (smooth) macroscopic observable F defined on the points x of the phase space $\mathcal{C}$, the time average of F exists for all μ_0-randomly-chosen initial data x and is given by

$$\lim_{M\to\infty} \frac{1}{M} \sum_{k=0}^{M-1} F(S^j x) = \int_{\mathcal{C}} \mu(\mathrm{d}x') F(x') \stackrel{\text{def}}{=} \langle F \rangle_+, \tag{1.1}$$

where μ is a S-invariant probability distribution on $\mathcal{C}$.

The chaotic hypothesis was essentially proposed by Ruelle in the case of fluid turbulence, and it is extended to non-equilibrium many-particle systems in [1]. If one assumes it, then it *follows* that the zeroth law holds, [5,6,8]; however, it is convenient to regard the two statements as distinct because the hypothesis we make is "*only*" that one can suppose that the system is Anosov for "practical purposes": this leaves the possibility that it is not strictly speaking such, and some corrections ("negligible in the thermodynamic limit") may be needed on the predictions obtained by using the hypothesis.

In the first references of [1] the generality of the hypothesis is discussed and in the second reference of [1], we derived, as a rather general consequence, predictions testable at least by numerical or physical experiments in systems with few degrees of freedom. The feature of the prediction relevant for numerical experiments, a *large deviation theorem* or *fluctuation theorem*, is that it is *parameter free*; other results concern the Onsager reciprocity in various classes of mechanical systems [10], or fluid models [11].

The theory was developed to understand the results in [12] which, therefore, provide also the *first* test. In this paper we present the results of numerical experiments that we conducted in order to check the hypothesis in models different from the shear flow model in [12].

Being a rather general principle, the chaotic hypothesis yields predictions that are sharp and *inescapable*, without free parameters. Hence it is important to check it with the highest precision possible. This immediately leads one to work at the limit of present day computer capability and to lengthy data elaboration.

In Section 2 we describe the models and give a quantitative description of their rough characteristics, discussing the experiments that we perform. In Section 3 we explain, through an analogy with well-known Ising model properties,

[2] One may wonder why we do not time observations at constant pace: this would indeed be possible. It is, however, convenient to time observations on natural events (i.e. using the jargon, "to make observations on a Poincaré's section") so that one eliminates one degree of freedom as well as the corresponding (trivially zero hence, strictly speaking, inconsistent with the chaotic hypothesis, because Anosov systems are hyperbolic) Lyapunov exponent, as recognized very early [13].

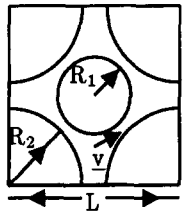

Fig. 1. General billiard structure with scatters of radius R_1 and R_2 in a periodic box with side length L (case $k \times l = 1 \times 1$).

the mechanism which allows us to acquire *exact* knowledge of some properties of μ without actually computing μ itself (which might be a surprising "achievement" if one does not examine in some detail, see the second reference of [1]). In Section 4 we present the raw experimental results; in Section 5 and in Appendix A we briefly summarize the methods followed in the statistical analysis of the results. In Section 6 we discuss interpretation problems of some suprising results obtained while performing various checks: in particular, one check is to verify that the number of positive Lyapunov exponents equals that of negative exponents, because this is a consequence of the chaotic hypothesis when the attractor is dense in phase space (a necessary condition for the fluctuation theorem to hold in the form of [1]). This turns out *not to be the case* in *one* of our four main experiments and we discuss the reasons why, nevertheless, the fluctuations theorem prediction holds within the errors. The analysis of Section 6 also presents comments and perspectives, and some challenging pictures that seem to emerge from our experiments and which led, after the present work was completed, to [10,14].

2. The models and a description of the experiments

The models contain thermostat mechanisms in order to enable the systems to reach a non-equilibrium stationary state in the presence of an imposed external field: therefore they are related to electrical conductivity problems. They represent a gas of N identical particles with mass m, interacting via a hard core *pair potential* φ with radius r and with an external potential $\varphi^e \neq 0$. The gas is enclosed in a two-dimensional box $[-\frac{1}{2}kL, \frac{1}{2}kL] \times [-\frac{1}{2}lL, \frac{1}{2}lL]$, $k, l = 1, 2, \ldots$, and is subject to periodic boundary conditions and to a horizontal constant external field $E_{\underline{i}}$ ($\underline{i}$ is a unit vector in the x-direction). The external potential will also be just a hard core interaction excluding access to the area covered by some obstacles or forbidding the crossing of the box walls. The obstacles are hard disks with centers situated on two square lattices with spacing L shifted by $\frac{1}{2}L$ relative to each other. The radii of the disks of each sublattice are equal and given by R_1 and R_2, respectively, so fixed that *every* rectilinear trajectory must suffer collisions with them. An alternative setting could have been a collection of identical hard disks (with large radii) with centers on a triangular lattice: the adopted geometry is the same as that of the previous paper [15].

The geometry is very simple and the position space is described in Fig. 1: The box $[-\frac{1}{2}kL, \frac{1}{2}kL] \times [-\frac{1}{2}lL, \frac{1}{2}lL]$ consists of $k \times l$ unit lattice cells with side L joined to form a square box: at the box boundary we impose priodic boundary conditions (*pbc*) or, alternatively, semiperiodic boundary conditions ($\frac{1}{2}$*pbc*): in the latter case the "horizontal" box walls was reflecting. The experiments with different boundary conditions have been performed "completely" independently, on different machines and with different codes.

The system is in contact with a "thermostat" which adds (or subtracts) energy so that the total internal energy stays rigorously constant. The equations of motion are:

$$\dot{\underline{q}}_j = \frac{1}{m}\underline{p}_j, \quad \dot{\underline{p}}_j = \underline{F}_j + E\underline{i} - \alpha(\underline{p})\underline{p}_j, \qquad \underline{F}_j \equiv -\sum_{i \neq j} \partial_{\underline{q}_j} \varphi(\underline{q}_j - \underline{q}_i) - \partial_{\underline{q}_j} \varphi^e(\underline{q}_j) \tag{2.1}$$

with $j = 1, \ldots, N$; $\alpha(\underline{p}) = E\,\underline{i}\cdot\sum_j \underline{p}_j/(\sum_j \underline{p}_j^2)$ and $\underline{F}_j$ is the (implusive) force acting on particle j (which is due only to the hard cores). The α–term incorporates the coupling to a "Gaussian thermostat" and it is assumed to obey Gauss' "principle of least constraint", see [16]. The constraint here is the constancy of the internal (i.e. kinetic) energy:

$$H(\underline{p},\underline{q}) = \sum_{i=1}^{N} \frac{\underline{p}_i^2}{2m} \stackrel{\text{def}}{=} e_0 N, \tag{2.2}$$

a typical non-holonomic constraint; it follows then from Gauss' principle that the force corresponding to the constraint is proportional to the gradient with respect to $\underline{p}_j$ of H. This model has been studied in great detail, in [17], in the case $N = 1$; a similar model has been investigated numerically in [18], and very recently in [19,20]. It is part of a wide class of models, see the second reference of [1], whose interest in the theory of non-equilibrium stationary states was pointed out in [21,22], where one can find the first studies performed in the context in which we are interested.

The timing events that we choose to follow are simply the collisions; whether with the walls or with the obstacles or with other parties. The boundary conditions will be periodic in both directions or reflecting in the one perpendicular to the field ("vertical") and periodic in the other ("horizontal").

The initial data will be fixed by a random choice with absolutely continuous distribution on the full phase space $\mathcal{F}$ (i.e. on the full energy surface).

The dimension of the phase space $\mathcal{F}$ of this system is that of the energy surface, i.e. $4N-1$, and that of the set of timing events $\mathcal{C}$ is $2D$ with $D = 2N-1$, i.e. one unit less than the dimension of $\mathcal{F}$. *The phase space "contraction" rate*, i.e. the divergence of the right-hand side of (2.1), is $\gamma(x) = D\alpha(x)$. It can be written in the form

$$\gamma(x) = D\alpha(x) = \frac{\epsilon(x)}{k_B T(x) + (2N/2D)(1/2m)\overline{\underline{p}}^2}, \tag{2.3}$$

where $\overline{\underline{p}} = (1/N)\sum_j \underline{p}_j$ is the average momentum, $\epsilon(x)$ the work done on the system per unit time by the external field and $\frac{1}{2}k_B T(x)$ is $(1/D)\sum_j (1/2m)(\underline{p}_j - \overline{\underline{p}})^2$ which, if k_B is Boltzmann's constant, defines the *kinetic temperature*: hence the name of *entropy production rate* per (kinetic) degree of freedom that will be occasionally given to $\alpha(x)$. Note that $\gamma(x)$ *does not have a definite sign*. In dimension $d \geq 2$ the factor $2N/2D$ would become $2N/dD$.

The above contraction corresponds to a contraction of the volume in the full phase space $\mathcal{F}$, between one collision and the next, given by $e^{-t_0\sigma(x)}$ with

$$\sigma(x) = \frac{1}{t_0}\int_0^{t(x)} \gamma(Q_t x)\,dt \tag{2.4}$$

if Q_t is the continuous time evolution (see Section 1) and t_0 denotes the *mean collision* time $t_0 = \langle t(\cdot)\rangle_+$.

We shall be concerned mostly with the contraction rate $\sigma_\tau(x)$ occurring during τ time steps as the system evolves between $S^{-\tau/2}$ and $S^{\tau/2}x$:

$$\sigma_\tau(x) \stackrel{\text{def}}{=} \frac{1}{\tau}\sum_{j=-\tau/2}^{\tau/2-1} \sigma(S^j x). \tag{2.5}$$

It has been proved [17] that for $N = 1$ and small $E \neq 0$ the average $\langle\sigma\rangle_+$ is positive, i.e. the system is *dissipative*. There seems to be no reason to think that $\langle\sigma\rangle_+$ is not positive when $N > 1$ and our experiments show that indeed this is the case.

Recently, in fact, it has been shown that under very general conditions (essentially under assumptions of smoothness and that the extended zero-th law holds) it must be $\langle\sigma\rangle_+ \geq 0$ [23]. In the latter paper it is also shown that $\langle\sigma\rangle_+ > 0$ if the SRB distribution μ gives probability 1 to set which has zero Liouville measure (i.e. if the attractor is "really" smaller than the full phase space)[3] and no Lyapunov exponent vanishes (note that smoothness zero-th law and no vanishing exponent hold if the system is Anosov, hance if the chaotic hypothesis is assumed).

Therefore it is natural to write

$$\sigma_\tau(x) = \langle\sigma\rangle_+ p(x) \tag{2.6}$$

so that the contraction of the phase space volume, while the system evolves between $S^{-\tau/2}x$ and $S^{\tau/2}x$, is $e^{-\tau t_o\langle\sigma\rangle_+ p(x)}$ and $\langle p\rangle_+ \equiv 1$.

In this case the time reversal map i defined by $i : (\underline{q}, \underline{p}) \to (\underline{q}, -\underline{p})$ is such that $\sigma_\tau(ix) = -\sigma_\tau(x)$.

The number $k \times l$ of unit lattice cells forming the box containing the gas will be called the *size* of the box. We define the *density* as $\rho = N/klL^2$ and the *energy density* as $e_0 = (1/N)\sum_j (1/2m)\underline{p}_j^2$ and we take units so that $m = 1, e_0 = \frac{1}{2}, L = 1$. The properties of the system are thus governed by the values of the parameters R_1, R_2, r and ρ; in place of ρ one could use the *occupied volume* $\delta = NV_0/(V - V_{\text{obs}})$, where V_0 is the particles volume, $V = klL^2$ the box volume and V_{obs} is the total volume of the obstacles, so that δ is the ratio between the volume occupied by the particle cores and the free volume where they can roam (i.e. the volume of the cell outside the volume V_{obs} occupied by the obstacles).

The field intensity E is fixed to $E = 1$ in all experiments. We shall consider systems with $N = 2$, $N = 10$, radii $R_1 = 0.2$, $R_2 = 0.4$ and $r = 0.005$ or $r = 0.01$ depending on the type of boundary conditions denoted, above, by *pbc* and $\frac{1}{2}$*pbc*. Here is a list of the above kinematic quantities in the cases that we shall consider:

Density	ρ	N/V
Energy density	e_0	$\frac{1}{2}$
Mass	m	1
Box side	L	1
Obstacles radii	R_1, R_2	0.2, 0.4
Particles radii	r	$0.005(pbc)$ or $0.01(\frac{1}{2}pbc)$
Occupied volume	δ	$NV_0/(V - V_{\text{obs}})$
Size	$k \times l$	$1 \times 1(pbc)$ or $2 \times 2(\frac{1}{2}pbc, N = 2)$ or $4 \times 5(\frac{1}{2}pbc, N = 10)$
Particle number	N	2 or 10

The following *dynamical* quantities are particularly interesting for the qualitative picture of the motions:

- The *average timing* t_0 of the collisions, equal to the future average $\langle t(\cdot)\rangle_+$ of the time $t(x)$ elapsing between two successive collisions.
- The *collision rate* ν will be the number of collisions between moving particles divided by the total number of collisions including the ones with the obstacles and the walls (the latter are present only in the $\frac{1}{2}pbc$ case).
- The *average entropy creation per collision*, equal to the future average $t_0\langle\sigma\rangle_+$.
- The *Lyapunov* exponents $\lambda_{\max}$ and $\lambda_{\min}$ defined, respectively, by the largest expansion rates of the elements under the action of the positive iterates of the evolution map S or by the minimum absolute value of the expansion or contraction rates.

[3] We call *attractor* a set G with minimal (Hausdorff) dimension which has the property that $\mu(G) = 1$, i.e. which has probability 1 in the stationary state. In general the closure clos(G) of the attractor may be the whole space $\mathcal{C}$ while the dimension of G may be much less.

- The entropy correlation time defined by the decay rate $\langle \sigma_\tau(S^n x)\sigma_\tau(x)\rangle_+ = \mathrm{O}(\mathrm{e}^{\vartheta n})$ of the entropy autocorrelation (recall that Q_t denotes the continuous time evolution, see Section 1), see [15,24] for an discussion of how reasonable it is to expect an exponential decay rate.

The data below have been obtained empirically, i.e. without any attempt at estimating errors, and are useful to get an idea of the basic qualitative properties of the system. For $N = 2$ particles with $e_0 = \frac{1}{2}$, $m = L = 1$, $E = 1$, density, k, l, and radii as above:

		$pbc, k = 1$	$\frac{1}{2}pbc, k = 2$
ρ	Density	2	0.5
δ	Occup. vol.	4.23×10^{-4}	4.23×10^{-4}
$\lambda_{\max}^{-1}$		1.32	1.31
$\lambda_{\min}^{-1}$		1.53×10^{1}	2.16×10^{1}
ϑ^{-1}	$\forall\tau$	≤ 20	≤ 20
t_0	Timing pace	1.50×10^{-1}	1.35×10^{-1}
ν	Collision rate	1.09×10^{-2}	4.93×10^{-3}
$\frac{t_0}{2N-1}\langle\sigma\rangle_+$	$\frac{\text{Entropyprod.}}{\text{Deg. freedom}}$	1.75×10^{-2}	1.49×10^{-2}

(2.7)

where only the errors (not shown, but amounting to less than 0.1%; see below) on t_0, $\langle\sigma\rangle_+$ have been measured with care since we need them in our experiments. The other data are purely indicative of the orders of magnitude; $\forall\tau$ means for all values of τ considered below.

For 10-particle systems we chose very different densities, for the cover with the test some "extreme" cases:

		$pbc, k = 1$	$\frac{1}{2}pbc, k = 2$
ρ	Density	10	0.5
δ	Occup. vol.	2.11×10^{-3}	4.23×10^{-4}
$\lambda_{\max}^{-1}$		3.50	4.71
$\lambda_{\min}^{-1}$		3.12×10^{2}	2.20×10^{3}
ϑ^{-1}	$\forall\tau$	< 20	< 20
t_0	Timing pace	2.87×10^{-2}	2.8×10^{-2}
ν	Pair collision	8.95×10^{-2}	8.92×10^{-3}
$\frac{t_0}{2N-1}\langle\sigma\rangle_+$	$\frac{\text{Entropy prod.}}{\text{Deg. freedom}}$	4.07×10^{-3}	3.52×10^{-3}

(2.8)

with the same comments on the errors and the symbols as presented in (2.7).

We shall study the probability distribution $\pi_\tau(p)\,\mathrm{d}p$, *in the stationary state* μ, of the variable p that is defined by (2.5) above for τ large. In fact the theory of the chaotic hypothesis foresees that, if τ is large compared to $\lambda_{\min}^{-1}$, then $\pi_\tau(p)$ verifies

$$\log\frac{\pi_\tau(p)}{\pi_\tau(-p)} = \tau t_0\langle\sigma\rangle_+ p. \tag{2.9}$$

This is the content of the *fluctuation theorem* discussed in [1,2,25] and it means that the *odd* part of $\log\pi_\tau(p)$ is linear in p with an a priori determined slope. *Nothing* is known about the *even* part.

One may think that the even part of proportional to p^2, i.e. $\log(\pi_\tau(p)/\pi_\tau(1)) = -\frac{1}{4}(p-1)^2\tau t_0\langle\sigma\rangle_+$; therefore it is interesting to check whether the *kurtosis*

$$\kappa_\tau = \frac{\langle (p-1)^4 \rangle_+ - 3\langle (p-1)^2 \rangle_+^2}{\langle (p-1)^2 \rangle_+^2} \tag{2.10}$$

vanishes if $\langle\cdot\rangle_+$ denotes average with respect to the SRB distribution μ in (1.1) (recall that $\kappa_\tau \equiv 0$ for a Gaussian distribution and the value κ_τ can be taken as a quantitative dimensionless estimate of the "non-gaussian" nature of the distribution). The central limit theorem for transitive Anosov systems [5] implies a Gaussian distribution for the variable σ_τ for large τ; this yields information about the deviations of $\tau\sigma_\tau$ from its average $\tau\langle\sigma\rangle_+$ by quantities of order $\sqrt{\tau}$ but (2.9) describes properties of *large deviations*, proportional to τ. Therefore there is no a priori reason to expect that the $\pi_\tau(p)$ is Gaussian; hence we *do not expect* that $\kappa_\tau = 0$; and the evaluation of κ_τ, once (2.9) is established, is of considerable interest.

Note that the variable σ_τ varies on a finite range, at fixed N. This means that p varies in a finite interval $[-p^*, p^*]$, symmetric by the time reversal symmetry, whose size can be easily measured and an idea of its value can be obtained from the following rough data for $\tau = 20$:

	$pbc, N = 2$	$\frac{1}{2}pbc, N = 2$	$pbc, N = 10$	$\frac{1}{2}pbc, N = 10$
p^*	9.91	9.25	7.92	8.55

(2.11)

that give the values of p^* on the actually observed trajectories. The definition of α and (2.4), by using the Schwartz inequality, imply a bound

$$p^* \le \frac{2N-1}{\langle\sigma\rangle_+} \frac{E}{\sqrt{2e_0}} \frac{t_{\max}}{t_0} \tag{2.12}$$

if e_0 is the energy per particle and $t_{\max}$ is the maximum time between collisions. Also the bound is saturated when all the particles have the same velocity parallel to the field.

Finally result (2.9) is valid in the *limit* $\tau \to \infty$ and this means that, in order to check it, one has to perform many experiments with various values of τ: one expects that τ should be large compared to ϑ^{-1}, *at least at fixed* p (but the errors are not expected to be uniform in p so that one should not be surprised to see still corrections at large values of p for values of τ for which (2.9) holds without appreciable corrections at small values of p).

In this experiment we have computed the distribution $\pi_\tau(p)$ at fixed τ (using the discrete evolution S) by measuring p over time intervals of length τ but *spaced by a fixed number of collisions* Δ during which no measurement is made. The time interval Δ has been taken large compared to the relevant characteristic times of the system, i.e. the average free flight time or the inverse of the time decay constant for the entropy autocorrelation function. The latter times being of the same order of magnitude and of the order of 1–10 collision times, we took $\Delta = 50$ collisions, see (2.7) and (2.8). Large Δ would have been better: but we would lose statistics. We then assume, in the statistical analysis, that the data so obtained are uncorrelated.

We made some empirical tests that this time delay was sufficiently large by investigating, in various cases, how important the time correlations were in the evaluation of the errors. Not unexpectedly we found that the statistical errors decrease by increasing the sampling delay Δ, in spite of the smaller statistical samples: so as far as statistical errors are concerned there is some (small) advantage in taking measurements spaced by Δ large. But mainly this was a test of our independence assumption used in the errors theory. If there had been a drastic change in the statistical errors, we would have concluded that the correlation time for the entropy production was not of the order of 10 collision times.

Another timescale of interest is $\lambda_{\min}^{-1}$: this is, however, very difficult to measure and it has value $+\infty$ for some values of E (see Fig. 9). There is no evidence that this timescale is related to the entropy autocorrelation: *which appears to be short ranged*, as far as we can see. On the other end there is evidence that as E grows the number of positive Lyapunov exponents decreases.

In Section 6 we try to establish a connection between this observation and the fluctuation theorem. This is very important for us as it leads to think that the chaotic hypothesis may hold in a far stronger sense than originally meant in the second reference of [1]. One can see that if the dimension of the stable manifold of the attractor points is not equal to that of the unstable manifold, then the closure of attractor for the forward motion cannot be the same as that of the attractor for the backward motion. Hence time reversal cannot leave the attractor invariant: *but* the chaotic hypothesis, as formulated in Section 1, tells us that *nevertheless* the motion *on the attractor* is reversible in the sense that there is a map i^* which leaves the attractor invariant and changes S into S^{-1}. The map i^* (whose existence is far from obvious) will be called the *local time reversal* on the attractor. As a consequence of this proposal, a scenario for an a priori explanation of the existence of i^* has been developed in [14] where the existence of i^* is linked to a general geometric property (called Axiom C: a global version of the notion of Axiom A).

3. Ising model analogy

The fluctuation theorem as expressed by (2.9) and the subsequent comments on the Gaussian nature of the function $\pi_\tau(p)$ may seem somewhat strange and unfamiliar.

It is therefore worth pointing out that the phenomenon of a "linear fluctuation law" on the odd part of the distribution, in the sense of (2.9), without a globally Gaussian distribution, is in fact well known in statistical mechanics and probability theory. Moreover, an example of what the fluctuation theorem means in a concrete case, in which $\pi_\tau(p)$ is *not* Gaussian, can be made by using the Ising model on a one-dimensional lattice Z.

We consider the space $\mathcal{C}$ of the *spin configurations* $\underline{\sigma} = \{\sigma_\xi\}, \xi \in Z$ and the map S that translates each configuration to the right (say). The "time reversal" is the map i: $\{\underline{\sigma}\} \to \{-\underline{\sigma}\}$ that changes the sign to each spin.

The probability distribution that approximates the SRB distribution is the finite volume Gibbs distribution:

$$\mu_\Lambda(\underline{\sigma}) = \frac{\exp(J\sum_{j=-T}^{t-1}\sigma_j\sigma_{j+1} + h\sum_{j=-T}^{T}\sigma_j)}{\text{normalization}}, \tag{3.1}$$

where $\Lambda = [-T, T]$ is a large interval, $J, h > 0$. The configuration $\underline{\sigma}$ outside Λ is distributed independently on the one inside the box Λ, to fix the ideas.

Calling $\langle m\rangle_+$ the average magnetization in the thermodynamic limit we define the magnetization in a box $[\frac{1}{2}\tau, \frac{1}{2}\tau]$ to be $M_\tau = \tau\langle m\rangle_+ p$ and we look at the probability distribution $\pi_\tau^T(p)$ of p in the limit $T \to \infty$. The Gibbs distribution corresponding to the limit of (3.1) will play the role of the SRB distribution. Calling this limit probability $\pi_\tau(p)$ it is easy to see that

$$\frac{\pi_\tau(p)}{\pi_\tau(-p)} \underset{\tau\to\infty}{\longrightarrow} e^{2\tau h\langle m\rangle_+ p}. \tag{3.2}$$

This is in fact obvious if we take the two limits $T \to \infty$ and $\tau \to \infty$ *simultaneously* by setting $T = \frac{1}{2}\tau$. In such a case, if $\sum_{\underline{\sigma};p}$ denotes summation over all the configurations with given magnetization in $[-T, T]$, i.e. such that $\sum_{j=-\tau/2}^{\tau/2-1}\sigma_j = \langle m\rangle_+ p$ the distribution (3.1) gives us immediately that

$$\frac{\pi_\tau^T(p)}{\pi_\tau^T(-P)} = \frac{\sum_{\underline{\sigma},p}(\exp J\sum_{j=-T}^{T-1}\sigma_j\sigma_{j+1} + h\sum_{j=-T}^{T}\sigma_j)}{\sum_{\underline{\sigma},-p}\exp(J\sum_{j=-T}^{T-1}\sigma_j\sigma_{j+1} + h\sum_{j=-T}^{T}\sigma_j)} \equiv e^{2\tau h\langle m\rangle_+ p} \tag{3.3}$$

if we use the symmetry of the pair interaction part of the energy under the "time reversal" (i.e. under spin reversal).

The error involved, in the above argument, in taking $T = \frac{1}{2}\tau$ rather than first $T \to \infty$ and then $\tau \to \infty$, can be easily corrected since the corrections are "boundary terms", and in one-dimensional short-range spin systems there

are no phase transitions and the boundary terms have no influence in the infinite volume limit (i.e. they manifest themselves as corrections that vanish, as $T \to \infty$ followed by $\tau \to \infty$).

One may not like that the operation i commutes with S rather than transforming it into S^{-1}. Another example in which the operation i does also invert the sign of time is obtained by defining i as $\{i\underline{\sigma}\}|_j = -\sigma_{-j}$: Eq. (3.3) can be derived also by using this new symmetry operation.

The above examples show why there is a priori independence between any Gaussian property of $\pi_\tau(p)$ and the fluctuation theorem. The theory of the fluctuation theorem in [1] is in fact *based* on the possibility (discovered in [5]) of representing a chaotic system as a one-dimensional short-range system of interacting spins (in general higher that $\frac{1}{2}$); and the argument is, actually, very close to the above one for the Ising model with, however, a rather different time reversal operation. See [25] for mathematical details on the boundary condition question.

4. Experimental results

Each of the measurements made is quite delicate and time consuming, hence the reader will probably forgive us for not having done all the experiments that one finds natural to do. Each experiment requires several days of CPU time on the computers that we used (and several months to prepare the final runs). The statistical errors have been measured by three times the standard deviation, and the other errors are estimated by following the criteria discussed in [15] and resumed in Appendix A. Thus the experiments *should be reproducible within our error bars* if the latter are defined as we do. Hopefully the data we give can be of use even if one decides (for mathematical reasons or to test other theoretical ideas) to change the assignments of the errors. In all the following graphs the error bounds are always marked although sometimes they may not be visible.

Since the results for the two boundary conditions are *very similar* (in spite of the density differences), including the error sizes we describe in detail only the cases of periodic boundary conditions which cover the two extreme densities considered. Other experiments at varying field intensity are described in Section 6.

4.1. $N = 2$ (*periodic boundary conditions*)

The values of R_1, R_2 are, respectively, 0.2, 0.4; the particle radius is 0.005 and the electric field is fixed $E = 1$, a value that seems to be quite large (see, however, Section 6). The qualitative data of the resulting evolution are given in the first column of Table (2.7).

4.1.1. *The probability distribution* $\pi_\tau(p)$

The evolution is studied over 1.08×10^6 collisions. In Fig. 2 we give the graph of $\pi_\tau(p)$ for various τ. The error bars are very small particularly for the data at the edge of the observability interval because the data are very many (and normalized). But the *relative errors* (not shown) are very small at the center and they are very large at the edges, of course.

We have attributed to each point on the above histograms a statistical error as explained in Section 5 (essentially they have been supposed independent variables and they have been given an error of three times the standard derivation). In fact the analysis of dispersion of each value shown that the "law of large numbers" is obeyed, and the standard deviation $m_n(\tau) \stackrel{\text{def}}{=} \langle (p - \langle p \rangle_\tau)^n \rangle$, $n = 2$, and the third-order deviation, $n = 3$, approach 0 with an apparent decay given by

$$m_2(\tau) = -0.005(\pm 0.002) + 39.80(\pm 0.05)\frac{1}{\tau}, \qquad m_3(\tau) = -0.002(\pm 0.004) + 93(\pm 1.5)\frac{1}{\tau^2}. \tag{4.1}$$

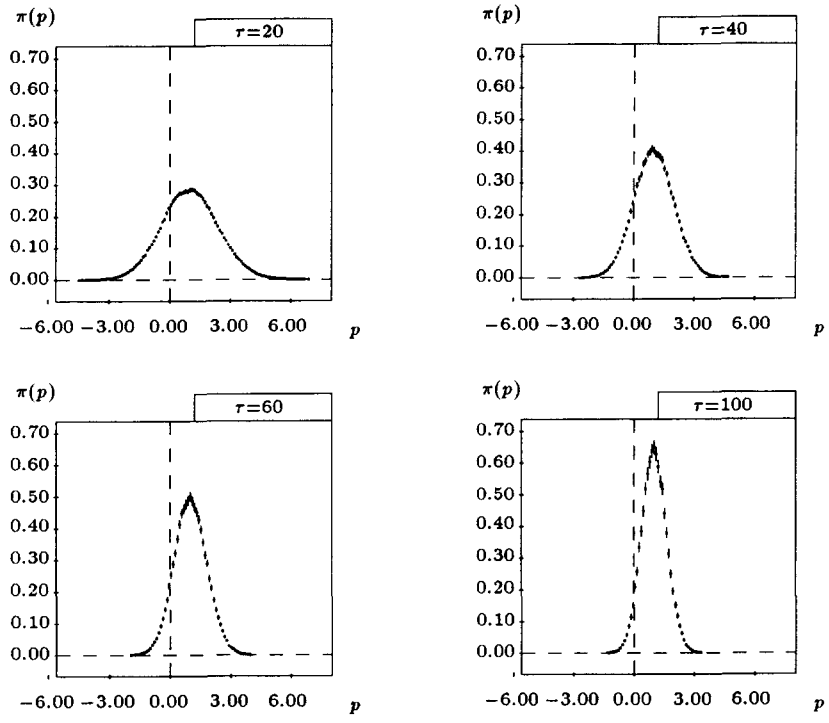

Fig. 2. The histograms for $\pi_\tau(p)$ at various values of the observation time $\tau = 20, 40, 60$ and 100. Each vertical bar is the error bar centered around the measured point. The dots on the axis mark the extremes of the interval where the observed data differ from 0 within the statistical error.

The error analysis leading to (4.1) follows the same scheme of [15]. We can also use here the notion of "goodness" introduced in [15] to measure how good a fit is (reproduced in Appendix A), and we measured the goodness of the above fits. We do not use the word "reliability test", and use the unusual "goodness" instead, to avoid inducing the reader to think that we rely on some sophisticated standard error analysis. The goodness is 2.45×10^{-3} and 4.94×10^{-3}, respectively.

The results are given in Fig. 3. The question of whether the probability distribution $\pi_\tau(p)$ is Gaussian is investigated by computing the *kurtosis* as a function of τ: the latter quantity defined in (2.10) can be fitted by a law

$$\kappa(\tau) = \left[0.00(\pm 0.01) + 2.3(\pm 0.3)\frac{1}{\tau}\right] \times \frac{1}{m_2(\tau)^2}. \tag{4.2}$$

The data are reported in Fig. 3. But, unlike the cases of $m_2(\tau)$ and $m_3(\tau)$ the goodness of this fit is 1.63×10^{-2} and it is *comparable* with the goodness of fits with a law $1/\tau^2$ or even $1/\tau^3$: the errors are too large so that many fits are "as good" (and also very good: this only shows that the notion of goodness has shortcomings as much as any other accuracy test).

We conclude that the distribution seems compatible with a Gaussian. Of course one expects a Gaussian behavior for the small deviations, i.e. for $(p - 1) \sim \tau^{-1/2}$: if one assumes that the system is Anosov (or just that it has an Axiom A attractor) then this follows, as a theorem, from the results of [5] (or [7]).

However, we know that it cannot be Gaussian beyond the range $O(\tau^{-1/2})$, because it has support between $\pm p^*$ with $p^* < +\infty$, see (2.11) and Section 3. Hence the apparent closeness to a Gaussian distribution might be an

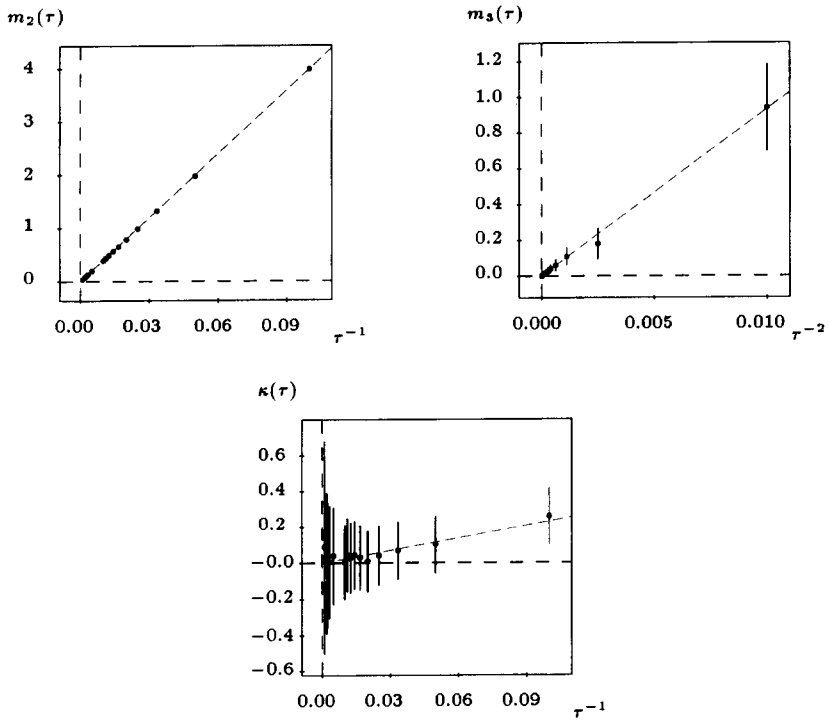

Fig. 3. The decay of the 2^d and 3^d moments, as functions of $1/\tau$ or $1/\tau^2$, and the kurtosis.

accident, that might disappear as τ increases. If it does not then this is an interesting question to examine, see Section 6.

In Fig. 4 we show the main quantity of interest here, i.e. the graph of

$$x(p) = \frac{1}{\tau t_0 \langle\sigma\rangle_+} \log \frac{\pi_\tau(p)}{\pi_\tau(-p)} \tag{4.3}$$

versus p (recall that $\langle\sigma\rangle_+$ is $(2N-1)j$ if j is the electric current).

The abscissae axis is discretized and the number of events in which p falls in a given interval is taken as proportional to $\pi_\tau(p)$. Therefore Fig. 4 is a histogram.

All values corresponding to different τ collapse on a single straight line in the interval $p \in [0, 1.5]$ in the worst cases (i.e. largest τ). For higher values of p (depending on τ) the statistics becomes gradually poorer as the deviations from the mean value of p become too large.

4.1.2. Conclusions

From the above data we infer that one cannot exclude that the distribution is Gaussian. *Assuming* that it is Gaussian then the fluctuation theorem *predicts* a standard deviation $m_2(\tau) = 2/\tau t_0 \langle\sigma\rangle_+ \equiv A/\tau$, see the lines preceding (2.10) and the above experimental data give:

$$\begin{aligned} A &= 37.96 \pm 0.21 \quad \text{(Gaussian assumption)}, \\ A &= 39.80 \pm 0.05 \quad \text{(experiment)}, \end{aligned} \tag{4.4}$$

where the Gaussian value is computed from the experimentally measured $\langle\sigma\rangle_+$ and t_0 (to which we attribute a statistical error of three times the standard deviation), while the experimental value is computed from $m_2(\tau)$, see (4.1); the error on the second line is as implied by (4.1).

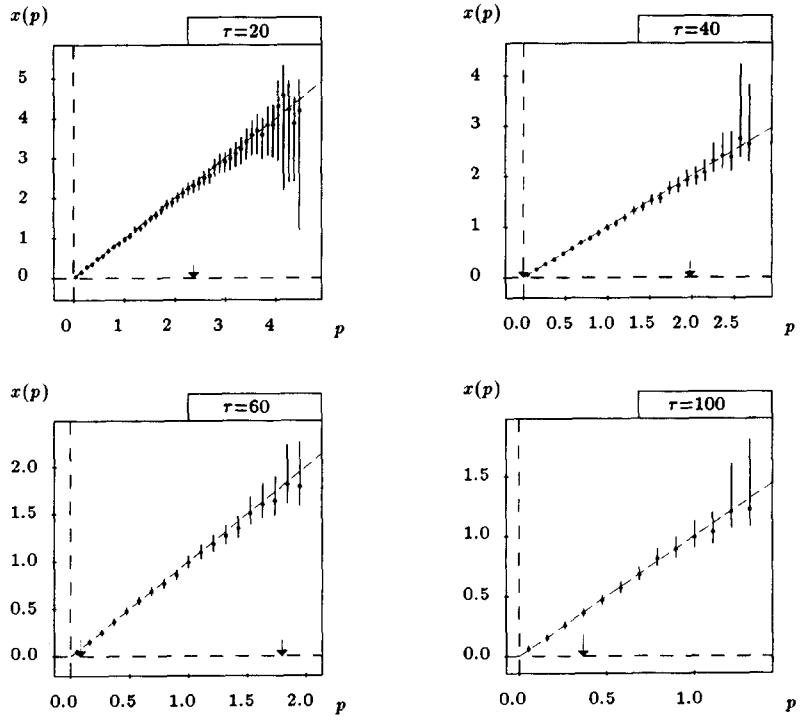

Fig. 4. The fluctuation theorem test for $\tau = 20, 40, 60$ and 100. The dashed straight line is the theoretical prediction of the fluctuation theorem. The arrows mark the point at distance $\sqrt{\langle (p-1)^2 \rangle}$ from 1. The error bars are inherited from the histogram data in Fig. 2.

The standard deviations of p from the value 1 are for $\tau = 20, 40, 60, 80$ and 100, respectively, 1.41, 0.99, 0.81, 0.70 and 0.63. Such values, multiplied by 3 (recall that our conventional statistical errors are three times the standard deviation), can be arbitrarily assumed to be the boundary between the small and the large deviations.

Note that, as already mentioned in Section 2, if the chaotic hypothesis is assumed then we know from the theory of Sinai that the small deviations obey a Gaussian law as $\tau \to \infty$: but the theory in general does not predict the standard deviation. The example of Section 3 is a good illustration, we believe, of the situation: in that case too we have a good understanding of the odd part of the distribution, but no grip on the even part and no reason to know a priori the distribution of the magnetization (i.e. also its even part). The results may mean that the values of τ that we reach are not large enough to test the validity of the central limit theorem. On the other hand the fluctuation theorem that follows from the chaotic hypothesis is *independent* of the central limit theorem (as the example in Section 3 suggests and illustrates) and therefore, the above results are, in our opinion, a good test of the chaotic assumption. We shall examine this point in more detail in Section 6.

Of course the choice, mentioned above, of three standard deviations to measure the statistical errors and the large deviations "threshold" is arbitrary. One could, as very often done, decide to use one standard deviation instead. Then we could say that we can go quite far in the large deviation region, but on the other hand many error bars become too small to be compatible with the data. This is a well-known problem with all experiments and we can just report that it appears also in the present experiment. It could only be solved by better experiments: hence we decided to perform experiments in which the computing facilities available to us were pushed further: the results of the (somewhat) more refined experiments were performed by using semiperiodic boundary conditions to extend the range of the test at the same time. The results did confirm the above picture and we do not discuss them in

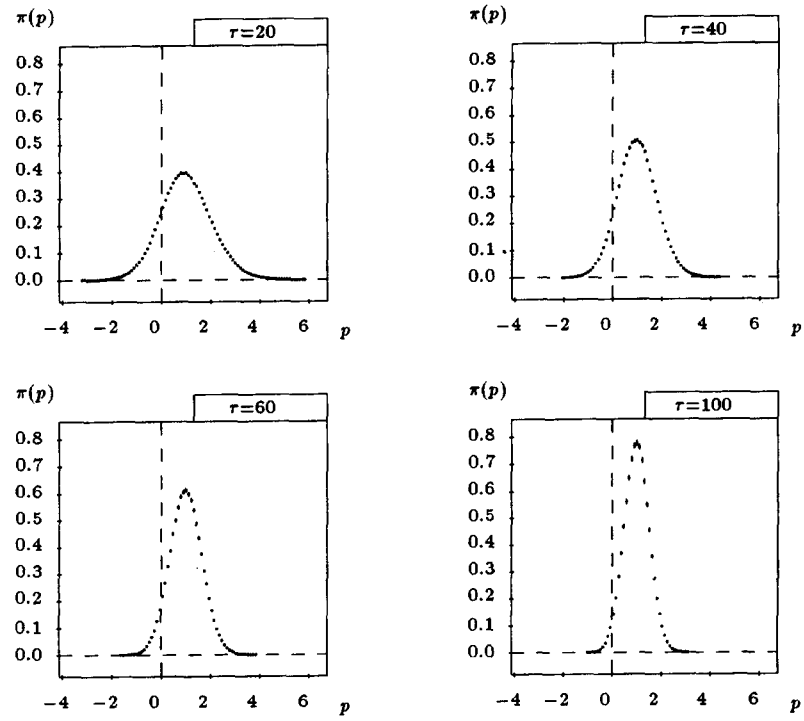

Fig. 5. The distribution $\pi_\tau(p)$ for $\tau = 20, 40, 60$ and 100.

detail: however, the new boundary conditions showed us an unexpected anomaly in the Lyapunov exponents, in the $N = 10$ case, of apparently minor importance for the purpose of the present discussion, but which stimulated (and in fact forced) us to widen considerably the scope of our investigations.

4.2. $N = 10$ (*periodic boundary conditions*)

The geometry is the same as in the previous case. The values of R_1, R_2 are, respectively, 0.2, 0.4; the particle radius is 0.005 and the electric field is fixed $E = 1$. The qualitative data of the resulting evolution are given in the first column of Table (2.8).

4.2.1. *The probability distribution* $\pi_\tau(p)$

The evolution is studied over 7.57×10^7 collisions. In Fig. 5 we give the graph of $\pi_\tau(p)$ for various τ, and in Fig. 6 we give the standard deviation and the third-order deviation, as in the previous case as functions of τ^{-1} and τ^{-2}, respectively.

The fits give

$$m_2(\tau) = 0.009(\pm 0.005) + 25.24(\pm 0.4)\frac{1}{\tau}, \qquad m_3(\tau) = -0.0002(\pm 0.0003) + 54.3(\pm 1.5)\frac{1}{\tau^2} \tag{4.5}$$

and the goodness of the above fits is 1.2×10^{-3} and 3.4×10^{-4}, respectively, for the data with $\tau > 25$. The data with $\tau < 25$ deviate from the above law and we interpret this as finite size effects (expected from the theory but absent in the previous case already for $\tau < 25$).

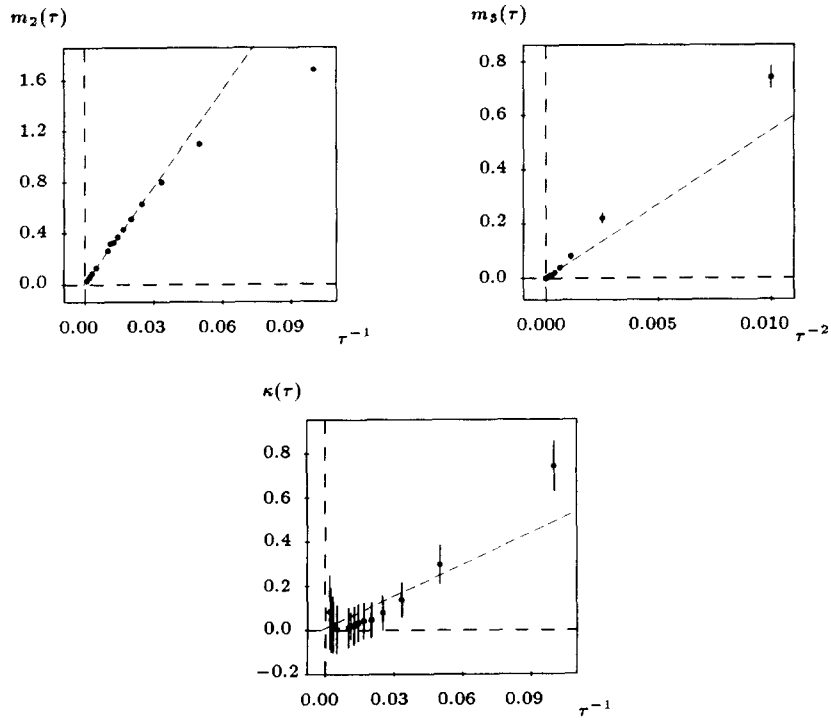

Fig. 6. The decay of the 2^d and 3^d moments, as functions of $1/\tau$ or $1/\tau^2$ and of the kurtosis as a function of $1/\tau$.

In Fig. 6 the kurtosis graph is reported for which we attempted a best fit as

$$\kappa(\tau) = -0.01(\pm 0.02) - 4.8(\pm 0.9)\frac{1}{\tau} \tag{4.6}$$

with a goodness of 4.03×10^{-4}. The data are not many because the experiment is hard (in terms of CPU time).

Finally the main quantity of interest, i.e. the graph of $x(p) = (1/\tau t_0 \langle\sigma\rangle_+) \log(\pi_\tau(p)/\pi_\tau(-p))$ versus p. The abscissae axis is discretized and the number of events in which p falls in a given interval is taken as proportional to $\pi_\tau(p)$. Therefore Fig. 7 is a histogram.

It is remarkable that the finite size effects, i.e. the manifestation of important deviations from the linear law for "small" τ (as we interpret them), are here very clear: the case $\tau = 20$ does not follow the scaling, in contrast to $\tau = 40, 60, 80, 100$ ($\tau = 80$ is not shown).

4.2.2. Conclusions ($N = 10$)

The case $N = 10$ is very similar to the case $N = 2$ as the theory predicts. From the above data we cannot exclude that the distribution is Gaussian in the observed range of values of p. *Assuming* that it is Gaussian then the theory gives a standard deviation $m_2(\tau) = 2/\tau t_0 \langle\sigma\rangle_+ \equiv A/\tau$, see (2.10) and the above experimental data give

$$\begin{aligned} A &= 25.82 \pm 0.02 \quad \text{(Gaussian assumption)}, \\ A &= 25.24 \pm 0.4 \quad \text{(experiment)}, \end{aligned} \tag{4.7}$$

where the theoretical value is computed from the experimentally measured $\langle\sigma\rangle_+$, t_0, while the experimental value is computed from the graphs for $m_2(\tau)$. The error analysis is carried along the same lines as that of the case $N = 2$ above.

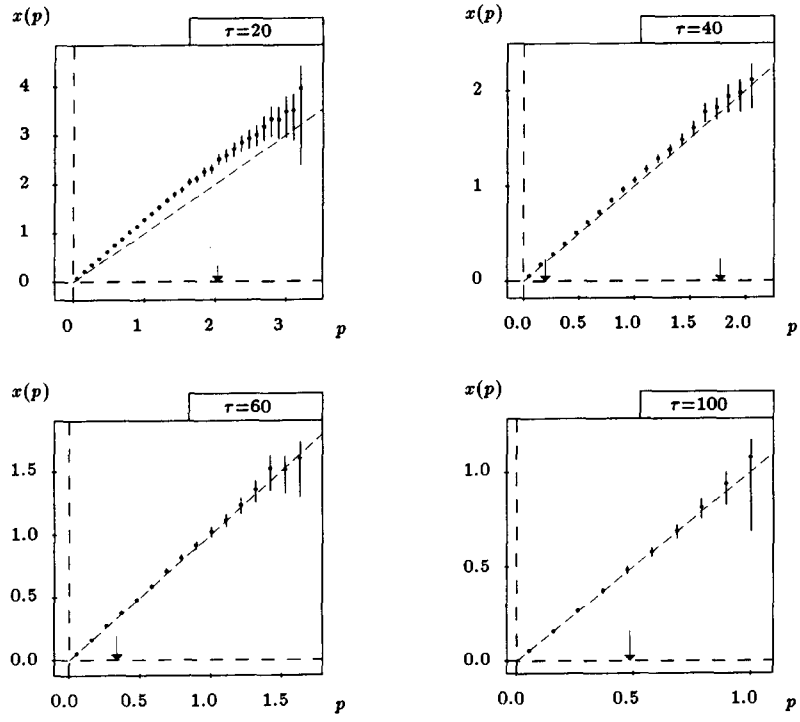

Fig. 7. The graphs for the fluctuation theorem test for $\tau = 20, 40, 60$ and 100. The dashed stright line is the theoretical prediction of the fluctuation theorem. The arrows mark the point at distance $\sqrt{\langle (p-1)^2 \rangle}$ from 1. The error bars are inherited from the histogram data in Fig. 5.

The standard deviations of p from the value 1 are for $\tau = 20$, 40, 60, 80 and 100 respectively $\sqrt{A/\tau} = 1.05$, 0.79, 0.66, 0.57 and 0.51. Such values, multiplied by 3, can be arbitrarily assumed to be the boundary between the small and the large deviations.

The same comments presented in the case $N = 2$ can be made here and therefore the data, in our opinion, yield a good test of the chaotic assumption in the case $N = 10$ too.

The same experiments have been performed in the case of semiperiodic boundary conditions: the results are so similar that we do not report their details. The reader can find them described in the preprints [26].

5. Error analysis of the distribution $\pi_\tau(p)$

A brief description of the methods that we use to define the errors follows. For a given τ, we build a time sequence of different p values

$$p_n \equiv p(x_{nt'}) = \frac{\sigma_\tau(x_{nt'})}{\langle \sigma \rangle_+^M}, \quad n = 1, \ldots, M, \tag{5.1}$$

where $x_{nt'} = S^{nt'}x, t' = \frac{1}{2}\tau + \Delta$ with x randomly chosen in phase space with absolutely continuous distribution and we have chosen $\Delta = 50$ in order to decorrelate contiguous evolution data points. The $\langle \sigma \rangle_+^M$ is fixed by normalization so that the property $M^{-1} \sum_{n=1}^M p(x_{nt'}) = 1$ holds, see (2.7).

That $\Delta = 50$ is a sufficient delay is warranted by the size of the entropy autocorrelation decay rate (denoted ϑ in Tables (2.7) and (2.8) Section 2). In general we would expect that Δ should be large compared to ϑ^{-1}. An accurate determination of ϑ (including a verification of the validity of an exponential law of decay, which is not a priori obvious: see the similar problems arising for the one particle case in [15]) is a major enterprise and we have only made a few empirical tests on the order of magnitude of ϑ: and our choice $\Delta = 50$ was dictated by purely numerical reasons as a reasonable compromise between small statistics, accuracy and computer availability. It is justified, in all our experiments, only by the empirically determined independence of the results (apart from the size of the errors) in the cases $\Delta = 20$ and $\Delta = 50$. We reported only the $\Delta = 50$ results.

We define the discrete probability distribution:

$$\pi_\tau^D(l; M) = \frac{\sum_{p_n \in I(l)} 1}{M}, \quad l = -100, \ldots, 100, \tag{5.2}$$

where $I(l) = [lr, (l+1)r]$ and $r = \frac{1}{10}$. The relation between the discrete and the continuous distribution when $M \to \infty$ is

$$\pi_\tau^D(l; \infty) = \int_{I(l)} \mathrm{d}p\, \pi_\tau(p). \tag{5.3}$$

Assuming that r is small enough we can expand the right-hand side of (5.3):

$$r^{-1}\pi_\tau^D(l; \infty) = \pi_\tau(lr + \tfrac{1}{2}r) + \frac{r^2}{24}\frac{\partial^2 \pi_\tau(p)}{\partial p^2}|_{p=lr+r/2} + \mathrm{O}(r^4). \tag{5.4}$$

We have checked that this $\mathrm{O}(r^2)$ correction is in all our cases negligible compared to other sources of error: this has been done by approximating in (5.3) the function $\pi_\tau(p)$ by a Gaussian distribution (which, a posteriori, is a good approximation to $\pi_\tau(p)$ in the range of p's that we study):

$$\pi_\tau(p) \simeq \frac{1}{\sqrt{2\pi}\sigma} \exp\left\{-\frac{(p-1)^2}{2\sigma^2}\right\}, \tag{5.5}$$

where $\sigma \equiv m_2$ is the experimental standard deviation of the distribution. By substituting (5.5) into the term with the second derivative in (5.4) we get

$$\pi_\tau(p) = r^{-1}\pi_\tau^D(l; \infty)\left\{1 - \frac{r^2}{24\sigma^2}\left[\frac{(p-1)^2}{\sigma^2} - 1\right] + \mathrm{O}(r^4)\right\} \tag{5.6}$$

with $p = lr + \frac{1}{2}r$.

We also have to estimate the error involved in approximating $\pi_\tau^D(l; \infty)$ by $\pi_\tau^D(l; M)$. Let us define

$$P_{\tau,l}(m; M) = \binom{M}{m} \pi_\tau^D(l; \infty)^m (l - \pi_\tau^D(l; \infty))^{M-m}, \tag{5.7}$$

where $P_{\tau,l}(m; M)$ is the probability that in M elements of a sequence there exists m in the interval defined by l. this means that we regard the various measurements of m as *independent*: because the empirical autocorrelation of the entropy production decays on scales smaller than Δ, the interval between successive measurements.

Then the average values of m and its mean square displacement are given by

$$\langle m \rangle_{\tau,l} = M\pi_\tau^D(l; \infty), \qquad \langle (m - \langle m \rangle_{\tau,l})^2 \rangle = \frac{\pi_\tau^D(l; \infty)[1 - \pi_\tau^D(l; \infty)]}{M}. \tag{5.8}$$

When M is large enough, we shall assume that

$$\pi_\tau^D(l;\infty) = \pi_\tau^D(l;M) \pm 3\left[\frac{\pi_\tau^D(l;M)(1-\pi_\tau^D(l;M))}{M}\right]^{1/2} \tag{5.9}$$

is an appropriate measurement of the error. Eqs. (5.6) and (5.9) are the relations used in the distribution analysis.

The error analysis of the fits for m_2, m_3, κ is the same as the one used in [15] and it is repeated, with some minor changes to adapt it to the present sistuations, in Appendix A.

6. Problems and further results (outlook)

(i) *Consistency and CODES:* The above experiments, see Figs. 4 and 6, seem in "good" agreement with the theoretical predictions, and as mentioned, we do not report (for brevity) the experiments performed in the case of semiperiodic boundary conditions because they simply confirm the agreement: see Fig. 10. We have attempted at a very accurate test compatibly with our computer resources and the need of a natural time cut-off on the experiments' duration. The only real limitation was the computer time available; not so much as available to us but to present day technology. By using the largest existing computers our results do not seem to be substantially improvable: the motion being chaotic there is not much that one can really do without really new ideas.

Our attitude is that the theory is general and it should apply to any system like the ones described in (2.1). So *in particular* to our computer programs, that we can refer to as the CODES. For such dynamical systems our experiments are, by definition, exact and the systems are also by construction "close" to (2.1).

Therefore on such grounds we could say that we can think that the only errors in our theory are the statistical errors, i.e. our experiment is as "perfect" as one could wish.

Nevertheless, not surprisingly, the situation is more subtle. The reason is mainly that we have been unable to write CODES which "solve" (2.1) (in "some sense", which is not very relevant for us here) and *at the same time verify the time reversibility property.*

This is a serious flaw: because the theory, see [1], *rests* on time reversal. Strictly speaking, then, we should apply the first part of the chaotic hypothesis and only assume that the attractor verifies Axiom A.

However, for this we have no theory: the only argument that one could give, and which we do not find convincing, is that the CODES are certainly "close" approximations to (2.1). Further, we are used to think that close systems behave closely. The abundance of counterexamples has not deterred people to have the feeling that there is some truth in such belief (*natura non-facit saltus*).

But since it might be simply impossible to write reversible, energy preserving, CODES what we have done looked to us to be the only possibility we had to test the principle.

It would be interesting to carry out experiments analogous to the above described ones for other types of systems for which reversible algorithms can be written and implemented at least in the conservative case, as discovered in [27]: it is unclear, however, if they can be extended to cover dissipative cases and, if so, if this can be done with the accuracy necessary to the test of the chaotic hypothesis.[4]

(ii) *The pairing rule, Axiom A attractors and reversibility:* If the chaoticity hypothesis, in the form given in Section 1 for the reversible case, is interpreted as meaning that the system behaves as a transitive Anosov reversible system, with the time reversal operation begin the "global time reversal" i, then the hypothesis implies that the

[4] The important paper [27] had escaped our attention until very recently, too late to take it into account: it proves that reversible codes do exist for systems not too far from ours and it is certainly important, and probably possible, to try to adapt them to test the chaotic hypothesis in a truly reversible CODE.

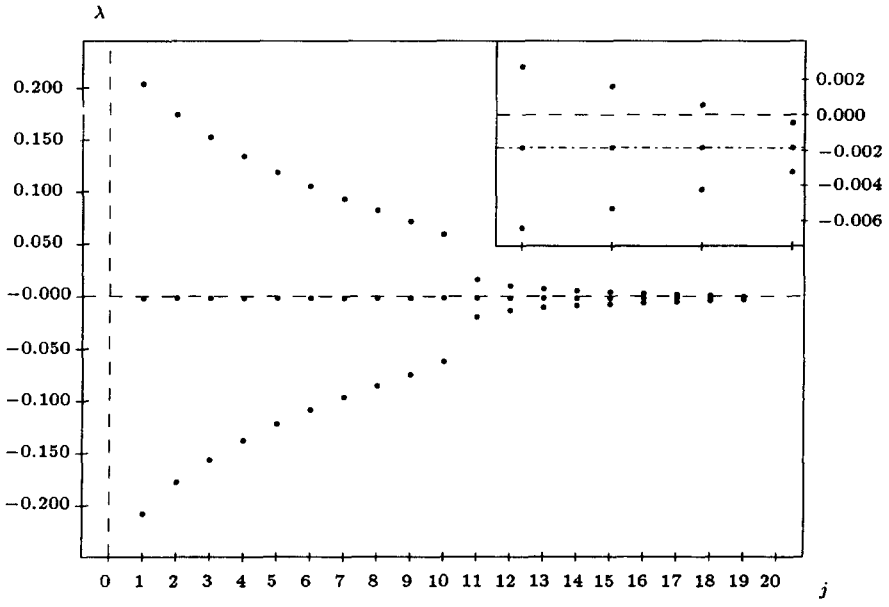

Fig. 8. The 38 Lyapunov exponents for 10 and $\frac{1}{2}(pbc)$. The small picture is an enlargment of the tail of the larger one and it shows more clearly the pairing rule and that the 19th exponent is slightly negative.

stable and unstable manifolds have the *same dimension*. So we would expect to have as many positive and negative Lyapunov exponents.

It was therefore natural to perform a "last" consistency check by measuring the Lyapunov exponents. This was necessary also because we became aware of the existence of the phenomenon in which, as E grows, some Lyapunov exponent that is > 0 at small E becomes < 0 at larger E: that this could happen while the system was still chaotic and at a not too large E-value was pointed out in [19]. Also tests showed, see Figs. 8 and 9, that in the case of 10 particles with *semiperiodic* boundary conditions the 19th (out of the 38) Lyapunov exponents is < 0.

The smallness of the 19th exponent in Fig. 8 may leave doubts about it being actually < 0. We think that the exponent *is* negative: however, the only method we know to estimate errors on the evaluation of Lyapunov exponents is by repeating many times the experiment. The amount of time (4 CPU days) per experiment explains why we did not do so (and why this is not done by other workers when studying such large systems): the errors on Lyapunov exponents are considered, in the literature, equal to the fluctuation of their partial values as the experiment proceeds. Of course we pushed the experiment until the fluctuation was comparable to 1 part in 10^3 so that such error would not be visible in Fig. 9.

We nevertheless performed, just for program testing purposes, several runs and the 19th exponent, *although fluctuating* from experiment to experiment, is systematically < 0 (while in the three other experiments, $N = 2$, 10 periodic and $N = 2$ semiperiodic, it is systematically positive).

A simple test to see how reliably we evaluate Lyapunov exponents can be, nevertheless, easily made: it consists in testing the *pairing rule*, discovered in [28,29], verified to an almost unthinkable accuracy in experiments by Dellago et al. [19], and recently *proved* for cases that include precisely our systems, see [20]. Although we did not push our study to check the pairing with the remarkable precision reached in [19], we find that the pairing rule is obeyed, see Fig. 8.

We stress, however, that the program we use to compute the Lyapunov exponents is very close (although not identical) to the actual scheme followed in [20] to *prove* the pairing rule. The proof shows that not only the Lyapunov

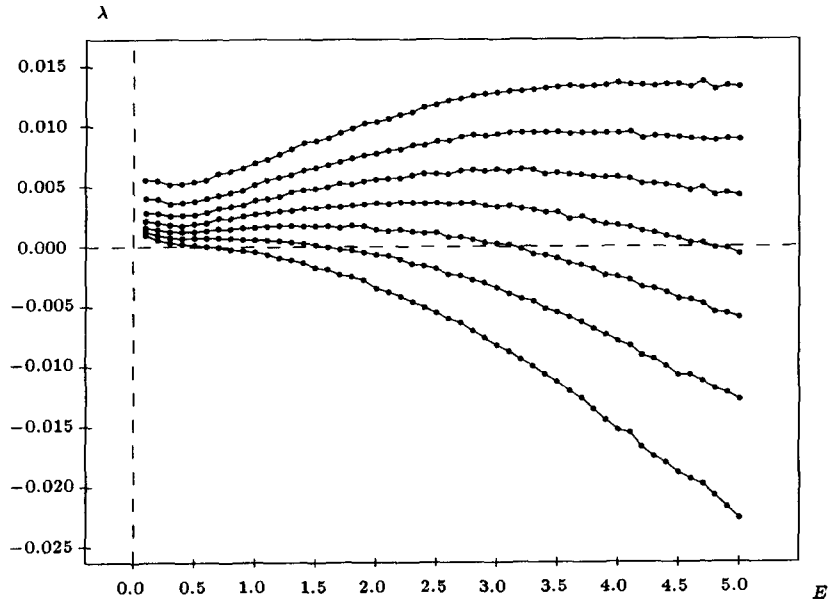

Fig. 9. The 13th through the 19th Lyapunov exponents in the case $N = 10$, $\frac{1}{2}(pbc)$: row data (no error bars estimated). The pairing rule [20,28,29,31] is verified.

exponents are paired but also their local values (that depend on the phase space point) extending what happens at $E = 0$, i.e. in the Hamiltonian case when the local exponents are trivially paired with 0 average. Hence the pairing rule has in fact to be fullfilled with high precision *even if the precision reached in measuring the exponents is not comparable to it* (in other words the errors that one makes on each exponent of a pair compensate exactly, see [20], if due to runs shortness).

The existence of one negative exponent (surprising for us, at the considered value of the field) in excess led us to study the question in more detail.

We first investigated whether this was a real effect (to clear doubts about it that could be raised by the difficulty to detect the sign of a small exponent). The experiment described below, see Fig. 9, shows that the effect is, in fact, *not at all delicate* and as the field E grows *certainly* many exponents "become" negative and as $E \to \infty$ even all of them may become negative (and the attrator would cease to be chaotic).

In fact, at least if there are not too many particles and the field is large, it might even be possible to prove the existence of a stable, periodic, attractor. In Fig. 9 is shown the graph of the Lyapunov exponents λ_j, with $j = 13$ to 19 in the $\frac{1}{2}$ *pbc* and 10 particles for $E = 0.1$ to $E = 5.0$ at steps of 0.1. The results are still "raw" in the sense that we have not yet been able to make a satisfactory study of the errors, for the same reasons as in the case $E = 1$. The computational method we used is the "usual method" [30] with a test trajectory of 0.5×10^5 collisions. The errors (defined as the fluctuations of the average quantities that should tend to the exponents values) are, however, quite large, and more accurate experiments are necessary to confirm the raw data (particularly for what concerns the absolute sizes of the exponents).

The preponderance of negative Lyapunov exponents over the positive ones does not seem due, at least in the cases where it appears clearly, to non-reversibility of our CODES (exponents do not change by varying the computations precision, within the limits of our experiments): hence existence of more negative than positive exponents is experimentally a real phenomenon at large E (and fixed N).

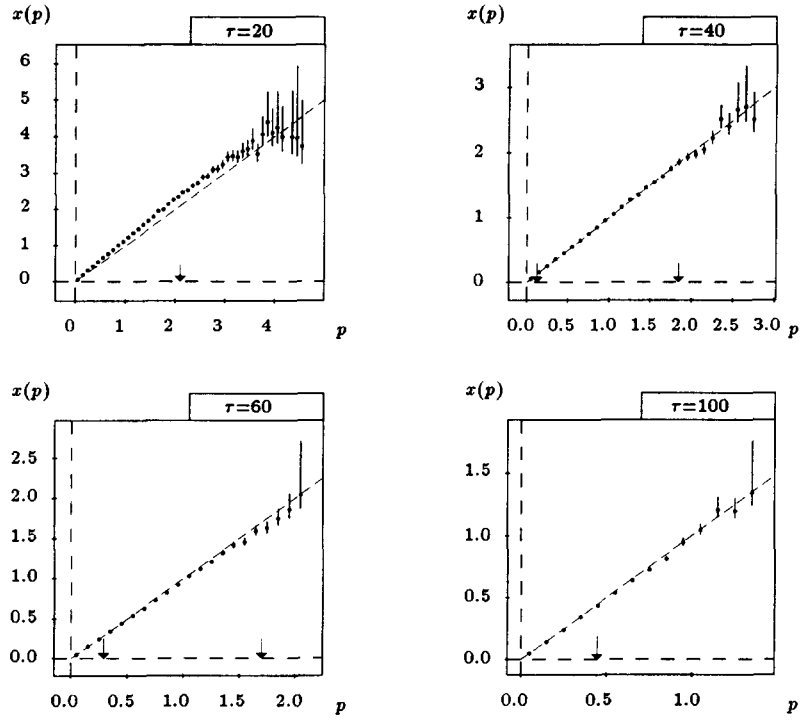

Fig. 10. The linear fluctuation test, $\tau = 20, 40, 80$ and 100. The dashed line is the fluctuation theorem prediction for $\tau = +\infty$. The arrows mark the point at distance $\sqrt{\langle (p-1)^2 \rangle}$ from 1.

Then one can ask: Is there any reason to think that the fluctuation theorem might hold even if the attractor is "only" an Axiom A attractor (i.e. with closure smaller than phase space)?

We have not been able to test the fluctuation law at values of E where there was an apparent excess of negative Lyapunov exponents (say at $E = 2.5$ in the case of 10 particles and $\frac{1}{2}(pbc)$ where we see two negative Lyapunov exponents in excess, see Fig. 9). The reason is that the estimated time for the corresponding numerical experiment is well beyond the present day computer capacities. Large fluctuations may be very difficult to observe at very large fields.

However, coming back to the case $E = 1$ of Fig. 8, it is a fact, illustrated in Fig. 10, that the fluctuation is consistent with the fluctuation theorem prediction.

The fluctuation law cannot hold by chance: but we see it well verified in a case where the experiments show one negative Lyapunov exponents in excess over the positive ones, see Fig. 10 giving the linear fluctuation test for $N = 10$, $\frac{1}{2}$ *pbc* (and Fig. 9 with $E = 1$).

This seems in conflict with the analysis given in the second reference of [1] whose validity appears very tightly related to the existence of a time reversal symmetry *leaving the closure of the attractor invariant*, i.e. a map i^* defined on the closure of the attractor and such that $Si^* = i^*S^{-1}$.

Therefore we conclude that a not unreasonable scenario would be that, when there are pairs of Lyapunov exponents consisting of two *negative* exponents, then the closure of the attractor can be simply regarded as a *smooth lower-dimensional surface.* [5] The motion on this lower-dimensional surface (whose dimension is smaller than that of phase

[5] This does not preclude the possibility that the attractor has a fractal dimension (smoothness of the closure of an attractor has nothing to do with its fractal dimensionality, see [1,2,32]).

space by an amount equal to the number of paired negative exponents) will still have an attractor (with dimension *lower* than the dimension of the surface itself, as suggested by the Kaplan–Yorke formula [32]). Moreover, on such lower-dimensional attracting manifold the motion will still be *reversible* in the sense that there will be a map i^* of the attracting manifold into itself (*certainly different from* the global time reversal map i) which *inverts* the time on the attractor and that can be naturally called a *local time reversal.*

Appropriate geometrical reasons for the existence of such local time reversal symmetry have later, stimulated by the present paper, been proposed and discussed, see [14]. The appearance of a non-time reversal invariant attracting manifold in a time reversible system can be regarded as *spontaneous symmetry breaking*: the existence of i^* means that in some sense time reversal cannot be broken: when it does spontaneously break then it is replaced by a lower symmetry (i^*) which "restores it". The analogy with the symmetries T (broken) and TCP (valid) of Fundamental Physics would be remarkable.

Then manifestly one would be back with an Anosov system (on a lower-dimensional manifold) and a version of the fluctuation theorem would still hold. Furthermore one could say that this is only a different interpretation of the chaotic principle of the second reference of [1] (which in such case does not even require to be reformulated to apply).

If this picture is correct, we can write the phase space contraction rate (see (2.3) and (2.4)) $\sigma(x) = \sigma_0(x) + \sigma_\perp(x)$ where $\sigma_0(x)$ is the contraction rate on the attracting surface on which the attractor lies and $\sigma_\perp(x)$ is the contraction rate of the part of the stable manifold of the attracting manifold points which is not on the manifold itself (the angle between the part of the stable manifold sticking out of the manifold and the manifold itself is disregarded here, as we think that is is bounded away from 0 and π since the attracting manifold is closed and bounded).

Of course local time reversal will change the sign *only of* $\sigma_0(x)$ and the fluctuation theorem should apply to the fluctuations of σ_0. But $\sigma_0(x)$ is *not* directly accessible to measurement: nevertheless we can still study its fluctuations via the following *heuristic* analysis. From the proof in [20] of the pairing rule one sees that the jacobian matrix J of the map S is such that $\sqrt{J^*J}$ has D pairs of eigenvalues and the logarithms of each pair add up to $\int_0^{t(x)} \alpha(Q_t x)\,dt$ (see also (2.3) and (2.4)).

The simplest interpretation of this, in view of the above proposed picture of the attractor, is that the pairs with elements of opposite signs describe expansion *on the attracting manifold.* While the $M \leq D$ pairs consisting of two negative eigenvalues describe the contraction of phase space in the directions *transversal to the attracting manifold.* Then, by the pairing rule, we would have $t_0\sigma_0(x) = (D - M)\int_0^{t(x)} \alpha(Q_t x)\,dt$ and we should have a fluctuation law for the quantity $p(x)$ associated with $\sigma_0(x)$ defined by (2.5) and (2.6) with σ_0 replacing σ, i.e. (accepting the above heuristic argument):

$$\sigma_{0\tau}(x) = \frac{(D - M)}{D}\langle\sigma\rangle_+ p(x), \tag{6.1}$$

i.e. a law identical to (2.9) *up to a correcting factor* $1 - M/D$:

$$\log\frac{\pi_\tau(p)}{\pi_\tau(-p)} = \tau t_0\langle\sigma\rangle_+\left(1 - \frac{M}{D}\right)p. \tag{6.2}$$

The graphs of Fig. 10 are relative to an experiment ($N = 10$ and semiperiodic boundary conditions) in which we see that there is one negative exponent in excess over the positive ones (as said above, see also Fig. 9): it is very small (see Fig. 8), and it carries an error bar that we estimate to be so large to allow for positive values as well. The graphs, however, show agreement with the experiment of Fig. 10 within the errors: had there been no negative exponents we would have expected a slope 1. If there is one negative exponent in excess, we expect a slope $1 - \frac{1}{19}$ which is within the error bars in Fig. 10 (had we drawn in Fig. 10 the best fit line rather than the line with slope 1

the agreement with the slope $1 - \frac{1}{19}$ would have been even better). But an excess of two exponents would yield a slope of $1 - \frac{2}{19}$ which is *out* of the error bars.

Note that since the exponent smallest in modulus is so small we may expect that it yields a clear effect only after extremely long times have elapsed (i.e. for values of $\tau > 4 \times 10^3$: totally out of computability).

The difficulty of the above scenario is that there is no a priori reason to think that attractors should have the above structure: i.e. fractal sets lying on smooth surfaces on phase space *on which motion is reversible*. But the picture is very suggestive and it might be applicable to more general situations in which reversibility holds only *on attractor closure* and not in the whole space (like "strongly dissipative systems"). As mentioned above a formal discussion of this point can be found in [14], which followed the completion of the present work.

(iii) *Smoothness of the closure of the attractor:* The smoothness of the surface on which the attractor lies, so that the attractor can be regarded, in itself, as an Anosov system, is very likely not necessary, from a mathematical viewpoint. The more general assumption that the attractor verifies Axion A (and is transitive) would be sufficient if accompanied by the (*very strong*) assumption that the attractor is mapped into itself by a symmetry i^* such that on the attractor $i^*S = S^{-1}i^*$ (discussed in (ii) above). We stress again that i^* *cannot be the same* as the global time reversal i because the latter will map the attractor for the forward motion into the one for the backward motion: however through simple examples of reversible motions with attractors closures smaller than the whole phase space (hence verifying Axion A but not the Anosov property) one can see that the existence of i often (always?) induces the existence of a map i^* on the attractor, see [14].

We insist in talking about smoothness for the following two reasons:

(1) Because we think that the theory applies to general many-particle systems and we cannot see the relevance of a possible fractional dimension over $N = 10^{19}$ total dimensions: in other words we can proceed as if the dimension was integer (in [1] the fractality is called "an unfortunate accident" that may happen in the problems that we study), hence as if the system is Anosov, *provided we accept that the attractor has a time reversal symmetry* (i.e. there is a map i^* of the attractor into itself that anticommutes with the time evolution, $S_t i^* = i^* S_{-t}$).

(2) Because, as it partially appears from Fig. 9, the Lyapunov exponents seem to evolve, as a function of E, along the following pattern. At smaller E they are all non-zero (as shown by Fig. 9): the dimension of the closure of the attractor in $4N - 2$ (i.e. that of the phase space C). Then as E grows one of them crosses continuously (and with non-zero E derivative, i.e. transversally) the value 0 at some $E_1 > 0$ becoming negative for larger values of the field; the closure of the attractor has now dimension $4N - 4$. At $E_2 > E_1$ a second Lyapunov exponent crosses 0 (transversally) and the closure of the attractor has now dimension $4N - 6$, etc. This suggests that, as E varies, the attractor is characterized by more and more "constants of motion", i.e. by the vanishing of more and more observables. Every time one more "constant of motion" is born we see that the attractor loses two dimensions. Nothing suggests to us that it becomes non-smooth, or appreciably so.

One should also bear in mind that the above analysis is, necessarily, carried over in systems with few degrees of freedom. It might well be that the picture can considerably simplify at large N. See below for some thoughts on that point.

(iv) *Fluctuation theorem as a reversibility test*: Since the very derivation [1,25] of the fluctuation theorem is so intimately related to reversibility one could say that if the predictions of the fluctuation theorem are verified, perhaps with a slope < 1 as suggested by (6.2), then this is a sign that the dynamics on the attractor is reversible in the sense that it is mapped into itself by a map i^* such that $i^*S = S^{-1}i^*$ (hence $i \neq i^*$ unless the system is Anosov and the attractor is the whole space). It is clear that the above considerations give rise to several tests that can be experimentally performed.

Note that not only the linearity in p is a strong statement, *but also the predicted value* < 1 *is somewhat surprising*: naively one could be tempted to think that the contraction rate transversal to the attractor is *uniform* over the attractor: this would lead to a slope > 1 (and the larger the stronger is the attraction from the attractor).

(v) *Gaussian? Central limit theorem?* One may say, as a first reaction to the analysis, "of course we expected a Gaussian distribution of the fluctuations because the dissipation $\tau\sigma_\tau$ is a sum of many terms that are statistically independent" if the motion is chaotic. Hence "everybody (reasonable)" would expect a Gaussian distribution for the fluctuations. But this would mean that $(p-1)$ has a dispersion of order $C\tau^{-1/2}$ for some (non-trivial) constant C related to the entropy autocorrelation function $\langle\sigma(S^n x)\sigma(x)\rangle$:

$$C^2 = \frac{1}{\langle\sigma\rangle_+^2}\sum_{n=-\infty}^{\infty}(\langle\sigma(S^n\cdot)\sigma(\cdot)\rangle_+ - \langle\sigma\rangle_+^2) \tag{6.3}$$

so that, calling $\zeta(p) = \lim_{\tau\to\infty}(1/\tau)\log\pi_\tau(p)$, the central limit theorem only implies that $\zeta'(1) = 0$, $\zeta''(1) = -C^{-2}$: this neither implies any relation between $\langle\sigma\rangle_+$ and C^2 nor it implies any large fluctuation property. On the other hand the fluctuation theorem tells us that $\zeta(p)$ has an odd part that is $\frac{1}{2}pt_0\langle\sigma\rangle_+$ so that

$$\log\frac{\pi_\tau(p)}{\pi_\tau(-p)} = \tau\langle\sigma\rangle_+ p \tag{6.4}$$

which, if the Gaussian distribution was assumed, would say that $t_0\langle\sigma\rangle_+ p = (2/C^2)p$ hence, *in general*, it would *also* be

$$\langle\sigma\rangle_+ = \frac{t_0}{2}\sum_{n=-\infty}^{\infty}(\langle\sigma(S^n\cdot)\sigma(\cdot)\rangle_+ - \langle\sigma\rangle_+^2). \tag{6.5}$$

The latter sum rule would be a *strange* (and *false* in our case, see below) prediction in the context of the central limit theorems where *no a priori relation* links the dispersion of a random variable and its average, in general.

Eq. (6.5) was found by us to be empirically verified, by examining the data in trying to understand a reason for the apparent Gaussian shape of $p \to \pi_\tau(p)$.

We then noticed the relation between (6.5) and the formula of Green–Kubo: i.e. that, as $E \to 0$, the two sides of (6.5) have both size of order $O(E^2)$ and the formula of Green–Kubo is the relation obtained by dividing the two sides by E^2 and letting $E \to 0$.

Once one sees that (6.5) reduces, in the lowest non-trivial order in E, to the formula of Green–Kubo then it becomes clear that the apparent Gaussian nature of the distribution $\pi_\tau(p)$ should rather be interpreted as a check of the (expected) approximate validity of (6.5). In the graphs of Figs. 2 and 5 the central peak should be Gaussian by the central limit theorem and (6.5) just shows that the dispersion of the Gaussian is compatible with the fluctuation theorem (at least for small field E) so that the deviations from the Gaussian cannot be seen near the center of the distribution and in the really large deviation region our errors are too large to detect non-Gaussian behavior (if (6.5) is approximately verified).

In the case $N = 1$ (6.5) was proved, to lowest non-trivial order in E, by Chernov et al. [17] to hold for values of E that, in our units, are *extremely small* compared to 1: the above argument is very general and it does not require small field (but reversibility is always needed).

The relation between chaotic hypothesis and the formula of Green–Kubo had been explicitly noted in [10] (see [10, Eq. (5.9)]): but the above argument leads to a conceptually different proof of it, based only on the fluctuation theorem (which however follows from the chaotic hypothesis). The latter fact is explicitly noted in [33] (where, of course, only the validity of (6.5) to lowest order in the fields was used): in [33] the above connection between (6.5) and the formula of Green–Kubo has been made precise and extended to more general systems with several external forces acting on them. This made it possible to see that the fluctuation theorem implies directly Onsager's reciprocity (for the reversible systems under consideration) and *can be interpreted as a nonlinear version of it.*

Still it is somewhat surprising that the distribution of p is sensibly Gaussian even at $E = 1$ which looks a very large field (it should be noted that if the N particles in the periodic box are considered as model for a crystal, with

N conduction electrons per cell, then the value $E = 1$ corresponds to an electric field of several millions of V/cm). Since the theory of the fluctuation theorem does not really give explicit error estimates (in our generality) on the remainders this does not raise any problem of principle ("how small is small"? i.e. which are the natural units for measuring the size of E?).

In the "old" literature one can, however, find statements that today sound somewhat mysterious like:

"It is empirically known that for macroscopic values of $\underline{\alpha}$, i.e. for values of the α_i much larger than their root mean square values at equilibrium, the averages of these quantities frequently obey linear differential equations."

which is then used to establish that relations between properties that hold for small fluctuations hold also for large ones, at least in the average. In [34, p. 100] the above statement is the beginning of a classical derivation of the Onsager reciprocity relations. Small and large fluctuations seem to have some common properties that one may not expect a priori or, at least, that one may consider worth of being challenged and tested, see [34, p. 102].

It is worth stressing again that we *know* that the distribution in p cannot be Gaussian for all p's: because there is a maximum (τ-independent) value that p can take, just from the finiteness of phase space. This value, called p^* in [25], can be easily measured in our experiments (see (2.11)) but it is very far away from the region where we have enough statistics to make meaningful measurements, as it appears from the graphs reported above.

(vi) *Timescales for large N:* A somewhat more speculative scenario can be drawn for large N. We mention it because we hope to receive some help in a program directed to test it. It seems reasonable to us that *in the thermodynamic limit* the system exponents will fall into two classes each consisting of a pair of exponents. The sum of the values of each pair is *constant* and equal to half the average entropy creation rate (this is the *pairing rule*, see above).

A large number of pairs (O(N)) will consist of one vanishing exponent and its negative companion. *The remaining postive Lyapunov exponents will all be identical: marking the timescale of local approach to equilibrium*, hence also the other negative exponents will be identical (by the pairing rule). By *identical* we mean here that the ratio between the largest and the smallest positive Lyapunov exponents is bounded uniformly in N (away from 0 and ∞).

This is in perfect agreement with Fig. 5 of [19] describing a *very high density system*: it is *not* in agreement with the other results of [19].

Nevertheless it is possible that the low density results are flawed in this respect as one would need far too large systems to obtain Lyapunov exponents for a distribution close to the thermodynamic limit distribution μ. Only in the high density case a small sample of gas exhibits the features of a large sample.

The above picture merges with the ideas in [11] relating the 0 Lyapunov exponents to the macroscopic modes described by macroscopic equations, while the non-zero exponents describe the approach to local equilibrium. It also matches with Fig. 8 where a rather sharp drop of the Lyapunov exponents towards 0 appears between 10th and 11th exponent.

Since it is always assumed that there is *only one microscopic timescale* for local approach to equilibrium it is perhaps a natural conjecture that Lyapunov exponents should have such structure.

(vii) *We see that the above experiments raise perhaps more problems than expected:* but the chaotic hypothesis emerges as not inconsistent with the data.

Appendix A. Fits and errors

This appendix is adapted to the present experiments from the corresponding appendix in [15]. We get data sets from our computer experiments, say $\underline{y}(\underline{x}) = \{y(x_i)\}_{i=1,N}$, where $\underline{x} = \{x_i\}_{i=1,N}$ is in our case an independent variable, say for instance a set of N collision numbers or time instants. To the latter experimental data set of points,

we want to *fit* a given *guessed* function, say $f(x;\underline{\alpha})$, where $\underline{\alpha} = \{\alpha_n\}_{n=1,p}$ is a set of arbitrary parameters. Here by fit we mean to find a set of parameters $\underline{\alpha}^*$ which *optimizes* some reasonable functional relation between the experimental data and the fitting function.

In our case we use the *least squares functional*, i.e.

$$V(\underline{y}(x),\underline{\alpha}) = \sum_{i=1}^{N}[y_i - f(x_i;\underline{\alpha})]^2. \tag{A.1}$$

The set of parameters $\underline{\alpha}^*(\underline{y})$ is here obtained by asking that they should be the minima of the V function: $\partial_{\underline{\alpha}^*} V(\underline{y},\underline{\alpha}^*) = 0$. We also define the *goodness* of our fit, G, by the average y-distance of our data to the function $f(x;\underline{\alpha}^*)$: $G(\underline{y}(\underline{x})) = (V(\underline{y}(\underline{x}),\underline{\alpha}^*)/N)^{1/2}$. This parameter is only meaningful when it is compared with the one from another fit. Given many fits, the one with smallest G value will be called *best fit* (among the considered fits).

The data have, in general, non-negligible errors, say $\underline{\varepsilon} = \{\varepsilon_i\}_{i=1,N}$, due to the finite number of samples used in the averaging (see comments in Section 2). Such errors induce errors on the parameter values. Therefore, a measure of the error amplitude in $\underline{\alpha}^*(\underline{y})$ is given by

$$\Delta_{\underline{\varepsilon}}\underline{\alpha}^*(\underline{y}) = \tfrac{1}{2}[\underline{\alpha}^*(\underline{y}+\underline{\varepsilon}) - \underline{\alpha}^*(\underline{y}-\underline{\varepsilon})]. \tag{A.2}$$

In the particular case in which the magnitude of the data error is much smaller than the measured value, $|\varepsilon_i/y(x_i)| \ll 1$, we may expand the latter equation around $\underline{\varepsilon} = \underline{0}$:

$$\Delta_{\underline{\varepsilon}}\alpha_n(\underline{y}) = \sum_{i=1}^{N} c_i^{(n)}(\underline{y})\varepsilon_i. \tag{A.3}$$

The coefficients $c_i^{(n)}$ are found by expanding $V(\underline{y}(\underline{x})+\underline{\varepsilon},\underline{\alpha})$ around $\underline{\alpha}^*(\underline{y})$ and $\underline{\varepsilon} = \underline{0}$ and, if $D_{mn} = \partial^2_{\alpha_m^*\alpha_n^*} V(\underline{y},\underline{\alpha}^*)$, they are given by

$$c_i^{(n)} = -\sum_{m=1}^{p} D^{-1}_{mn}\partial^2_{y(x_i)\alpha_m^*} V(\underline{y},\underline{\alpha}^*). \tag{A.4}$$

In particular for the linear fit, $f(x,\underline{\alpha}) = \alpha_1 + \alpha_2 x$, the coefficients $c_i^{(1),(2)}$ are given by

$$c_i^{(1)} = \frac{2}{N\Delta x}(\overline{x^2} - \overline{x}x_i), \qquad c_i^{(2)} = \frac{2}{N\Delta x}(x_i - \overline{x}), \tag{A.5}$$

where $\Delta x = \overline{(x-\overline{x}^2)^2}$ and $\overline{x^n} = N^{-1}\sum_{i=1}^{N} x_i^n$.

The errors are random variables and we have to average them over their distribution. In all cases considered it seemed reasonable to consider the errors ε_i as independent variables. Therefore we *empirically* estimate an upper bound for their correlation values:

$$|\langle\varepsilon_i\varepsilon_j\rangle| \le \sqrt{\langle\varepsilon_i^2\rangle\langle\varepsilon_j^2\rangle}. \tag{A.6}$$

The parameter errors in our analysis are defined by the equation

$$\Delta\alpha_n(\underline{y})^2 = \sum_{i=1}^{N}\sum_{j=1}^{N} c_i^{(n)}c_j^{(n)}\delta_i\delta_j \ge \langle\Delta_{\underline{\varepsilon}}\alpha_n^2\rangle, \tag{A.7}$$

where $\delta_i^2 = \langle\varepsilon_i^2\rangle$ and their use and meaning is described entirely by the above comments.

Acknowledgements

We are indebted to E.G.D. Cohen for his interest and his comments and suggestions: his constant support and advice have been very important to us. We thank J. Lebowitz and D. Ruelle for many discussions during which they provided inspiration and ideas. This work is part of the research program of the European Network on: "Stability and Universality in Calssical Mechanics", # ERBCHRXCT940460, and it has also been partly supported by Rutgers University, CNR-GNFM, IHES and MPI.

References

[1] G. Gallavotii and E.G.D. Cohen, Dynamical ensembles in nonequilibrium statistical mechanics, Phys. Rev. Lett. 74 (1995) 2694–2697; Dynamical ensembles in stationary states, J. Statist. Phys. 80 (1995) 931–970.
[2] G. Gallavotti, Topics in chaotic dynamics, Lectures at the Granada school 1994, eds. P. Garrido and J. Marro, Lecture Notes in Physics, Vol. 448 (Springer, Berlin, 1995) pp. 271–311.
[3] V. Arnold and A. Avez, Ergodic Problems of Classical Mechanics (Benjamin, New York, 1966).
[4] S. Smale, Differentiable dynamical systems, Bull. Amer. Math. Soc. 73 (1967) 747–818.
[5] Y.G. Sinai, Gibbs measures in ergodic theory, Russian Math. Surveys 27 (1972) 21–69; Lectures in Ergodic theory (Princeton University Press, Princeton, 1977).
[6] D. Ruelle, Chaotic motions and strange attractors, Lezioni Lincee, notes by S. Isola, Academia Nazionale dei Lincei (Cambridge University Press, Cambridge, 1989); see also D. Ruelle, Measures describing a turbulent flow, Ann. New York Academy Sci. 357 (1990) 1–9; for more technical expositions see D. Ruelle, Ergodic theory of differentiable dynamical systems, Publications Mathémathiques de l'IHES 50 (1980) 275–306.
[7] D. Ruelle, A measure associated with Axiom A attractors, Am. J. Math. 98 (1976) 619–654.
[8] R. Bowen, Equilibrium states and the ergodic theory of Anosov diffeomorphisms, Lecture Notes in Mathematics, Vol. 470 (Springer, Berlin, 1975).
[9] G.E. Uhlenbeck and G.W. Ford, Lectures in Statistical Mechanics (American Mathematical Society, Providence, RI) 1963, pp. 5, 16, 30.
[10] G. Gallavotti, Chaotic hypothesis: Onsager reciprocity and fluctuation–dissipation theorem, J. Statist. Phys., in press.
[11] G. Gallavotti, Chaotic principle: Some applications to developed turbulence, in mp_arc@math. utexas. edu, # 95-232 (1995).
[12] D.J. Evans, E.G.D. Cohen and G.P. Morriss, Probability of second law violations in shearing steady flows, Phys. Rev. Lett. 71 (1993) 2401–2404.
[13] E. Lorenz, A deterministic non-periodic flow, J. Atomospheric Sci. 20 (1963) 130–141.
[14] F. Bonetto and G. Gallavotti, Reversibility, coarse graining and the chaoticity principle, preprint, in mp_arc@math. utexas. edu, # 96-50.
[15] P. Garrido and G. Gallavotti, Billiards correlation functions, J. Statist. Phys. 76 (1994) 549–586.
[16] T. Levi-Civita and U. Amaldi, Lezioni di Meccanica Razionale, Zanichelli, Bologna, 1927 (reprinted 1974), Vols. I, II_1, II_2.
[17] N.I. Chernov, G.L. Eyink, J.L. Lebowitz and Y.G. Sinai, Steady stae electric conductivity in the periodic Lorentz gas, Comm. Math. Phys. 154 (1993) 569–601.
[18] A. Baranyai, D.T. Evans and E.G.D. Cohen, Field dependent conductivity and diffusion in a two-dimensional Lorentz gas, J. Statist. Phys. 70 (1993) 1085–1098.
[19] C. Dellago, H. Posch and W. Hoover, Lyapunov instability in system of hard disks in equilibrium and non-equilibrium steady states, preprint, Institut für Experimentalphysik, Universität Wien, Austria (August 1995).
[20] C.P. Dettman and G.P. Morriss, Proof of conjugate pairing for an isokinetic thermostat, N.S. Wales U., Sydney 2052, preprint (1995).
[21] B.L. Holian, W.G. Hoover and H.A. Posch, Resolution of Loschmidt's paradox: the origin of irreversible behavior in reversible atomistic dynamics, Phys. Rev. Lett. 59 (1987) 10–13.
[22] H.A. Posch and W.G. Hoover, Nonequilibrium molecular dynamics of a classical fluid, in: Molecular Liquids: New Perspectives in Physics and Chemistry, ed. J. Teixeira-Dias (Kluwer Academic Publishers, Dordrecht, 1992) pp. 527–547.
[23] D. Ruelle, Positivity of entropy production in nonequilibrium statistical mechanics, IHES preprint (1995).
[24] Artuso, G. Casati and Guarneri, J. Statist. Phys. (1995).
[25] G. Gallavotti, Reversible Anosov diffeomorphisms and large deviations Math. Phys. Electronic J. 1 (1) (1995).
[26] F. Bonetto, G. Gallavotti and P. Garrido, Archived in chao-dyn/964017 or mp_arc/96-154.
[27] D. Levesque and L. Verlet, Molecular dynamics and time reversibility, J. Statist. Phys. 72 (1993) 519–537.
[28] D.J. Evans, G.P. Morriss Statistical Mechanics of Nonequilibrium Liquids (Academic Press, New York, 1990).
[29] D.J. Evans, E.G.D. Cohen and G.P. Morriss, Viscosity of a simple fluid from its maximal Lyapunov exponents, Phys. Rev. 42 (1990) 5990–5997.

[30] G. Benettin, L. Galgani, A. Giorgilli and J.M. Strelcyn, Lyapunov characteristic exponents for smooth dynamical systems and for Hamiltonian systems; a method for computing all of them. Part 1: Theory, Meccanica 15 (1980) 9–20; Lyapunov characteristic exponents for smooth dynamical systems and for Hamiltonian systems; a method for computing all of them. Part 2: Numerical applications, Meccanica 15 (1980) 21–30.
[31] S. Sarman, D.J. Evans and G.P. Morriss, Conjugate pairing rule and thermal transport coefficients, Phys. Rev. A 42 (1992) 2233–2242.
[32] J. Eckmann, D. Ruelle Ergodic theory of strange attractor, Rev. Mod. Phys. 57 (1993) 617–656.
[33] G. Gallavotti, Extension of Onsager's reciprocity to large fields and the chaotic hypothesis, mp_arc 96-109; or chao-dyn 9603003.
[34] S. de Groot and P. Mazur, Nonequilibrium thermodynamics (Dover, New York, 1984).